NeuroImage: Clinical 13 (2017) 428–438

Contents lists available at ScienceDirect

NeuroImage: Clinical

journal homepage: www.elsevier.com/locate/ynicl

Primary visual cortical remapping in patients with inherited peripheral retinal degeneration

Sónia Ferreira[a], Andreia Carvalho Pereira[a], Bruno Quendera[b], Aldina Reis[a,c], Eduardo Duarte Silva[a], Miguel Castelo-Branco[a,b,*]

[a] Visual Neuroscience Laboratory, Institute for Biomedical Imaging and Life Sciences (CNC.IBILI), Faculty of Medicine, University of Coimbra, 3000-548 Coimbra, Portugal
[b] Institute of Nuclear Sciences Applied to Health (ICNAS), Brain Imaging Network of Portugal, University of Coimbra, 3000-548 Coimbra, Portugal
[c] Ophthalmology Unit, Centro Hospitalar e Universitário de Coimbra (CHUC), 3000-075 Coimbra, Portugal

ARTICLE INFO

Article history:
Received 31 July 2016
Received in revised form 10 November 2016
Accepted 14 December 2016
Available online 21 December 2016

Keywords:
Functional magnetic resonance imaging (fMRI)
Human
Retinitis pigmentosa
Plasticity
Reorganization
Primary visual cortex
Retinotopy

ABSTRACT

Human studies addressing the long-term effects of peripheral retinal degeneration on visual cortical function and structure are scarce. Here we investigated this question in patients with Retinitis Pigmentosa (RP), a genetic condition leading to peripheral visual degeneration. We acquired functional and anatomical magnetic resonance data from thirteen patients with different levels of visual loss and twenty-two healthy participants to study primary (V1) visual cortical retinotopic remapping and cortical thickness. We identified systematic visual field remapping in the absence of structural changes in the primary visual cortex of RP patients. Remapping consisted in a retinotopic eccentricity shift of central retinal inputs to more peripheral locations in V1. Importantly, this was associated with changes in visual experience, as assessed by the extent of the visual loss, with more constricted visual fields resulting in larger remapping. This pattern of remapping is consistent with expansion or shifting of neuronal receptive fields into the cortical regions with reduced retinal input. These data provide evidence for functional changes in V1 that are dependent on the magnitude of peripheral visual loss in RP, which may be explained by rapid cortical adaptation mechanisms or long-term cortical reorganization. This study highlights the importance of analyzing the retinal determinants of brain functional and structural alterations for future visual restoration approaches.

1. Introduction

Plasticity or reorganization refers to the brain propensity to change its structural or functional connectivity in response to environmental demands. The ongoing debate on the nature of the plastic modifications induced by retinal diseases evolving after the critical period of neural development remains to be settled (Espinosa and Stryker, 2012; Martins Rosa et al., 2013; Merabet and Pascual-Leone, 2010; Pascual-Leone et al., 2005; Thomas and Baker, 2013; Wandell and Smirnakis, 2009).

Retinitis Pigmentosa (RP) is an inherited progressive degeneration of photoreceptors, starting at the periphery and advancing progressively towards the central retina. Onset age varies from infancy to adulthood. Clinical manifestations include night blindness, tunnel vision, and eventually full blindness in advanced stages (Hamel, 2006; Musarella and Macdonald, 2011). Human studies concerning the effects of peripheral visual loss on visual cortical function are scarce. The majority of previous studies have addressed central visual disorders such as macular degeneration. Given that peripheral and central vision are distinctly processed in the brain (Burnat, 2015; Wang and Yamamoto, 2013), mechanisms of spatial reorganization might be different depending on whether central or peripheral vision degenerates, warranting the need to study the impact of peripheral visual loss on brain plasticity.

A functional Magnetic Resonance Imaging (fMRI) study (Masuda et al., 2010) assessing three RP patients suggested that task-dependent changes in visual cortical responses may occur in regions corresponding to silent cortical zones matching patients' scotomata (retinal lesion areas) in primary visual cortex (V1) – the Lesion Projection Zone (LPZ). That study proposed that response-dependent unmasking of feedback signals is driven from higher order visual areas. Another single

Abbreviations: RP, Retinitis Pigmentosa; MRI, Magnetic Resonance Imaging; fMRI, functional Magnetic Resonance Imaging; RNFL, Retinal Nerve Fiber Layer; LE, Left Eye; RE, Right Eye; LH, Left Hemisphere; RH, Right Hemisphere; FPZ, Function Projection Zone; LPZ, Lesion Projection Zone.

* Corresponding author at: IBILI, Faculty of Medicine, University of Coimbra, Azinhaga de Santa Comba, 3000-548 Coimbra, Portugal.
E-mail addresses: sonia.ferreira@fmed.uc.pt (S. Ferreira), aspereira@fmed.uc.pt (A.C. Pereira), bruno.alexandre.pq@gmail.com (B. Quendera), aldinareis@gmail.com (A. Reis), esilva2579@hotmail.com (E.D. Silva), mcbranco@fmed.uc.pt (M. Castelo-Branco).

http://dx.doi.org/10.1016/j.nicl.2016.12.013

case fMRI report of one RP patient found no evidence of functional reorganization in the cortical LPZ (Goesaert et al., 2014).

Contrasting with RP, macular degeneration mainly affects central vision. Some authors claimed that in this condition the deafferented central cortical neurons in V1 become responsive to inputs from the peripheral retina (Baker et al., 2008; Cheung and Legge, 2005; Dilks et al., 2014, 2009; Liu et al., 2010). However, other studies have questioned such visual cortical reorganization (Baseler et al., 2011b; Boucard et al., 2009; Goesaert et al., 2014; Lešťák et al., 2013; Plank et al., 2011; Sunness et al., 2004; Thibaut et al., 2014; Van der Stigchel et al., 2013).

It is important to point out that the association between structural and functional visual cortical reorganization is also poorly studied. To our knowledge, only two studies analyzed both functional and structural brain alterations due to retinal disorders in the same cohort, but only from a cross-modal plasticity point of view (Anurova et al., 2014; Büchel et al., 1998). In the first study, authors found a negative correlation between cortical thickness and functional activation during auditory tasks in occipital areas of early blind patients. In the second study, the visual cortical morphology in early and late blind patients was intact but functional activation was found during tactile and auditory tasks. Nonetheless, both studies focused on cross-modal plasticity mechanisms and not in characterizing simultaneously the structure and function of visual cortical regions in the context of specific changes triggered by a retinal disorder. Additionally, the majority of reports on structural changes combine several ophthalmological conditions involving distinct mechanisms, which may hinder the understanding of specific brain changes triggered by a particular disease (Anurova et al., 2014; Boldt et al., 2014; Dietrich et al., 2013; Erika et al., 2014; Lee et al., 2014; Lewald and Getzmann, 2013; Park et al., 2009; Plank et al., 2011; Renier et al., 2013; Wang et al., 2014; Weaver et al., 2013; Xie et al., 2012). Previous studies with advanced stage patients with glaucoma and macular degeneration (Bogorodzki et al., 2014; Boucard et al., 2009; Chen et al., 2013; Hernowo et al., 2014; Plank et al., 2011; Yu et al., 2014; Zikou et al., 2012) and blind participants (Anurova et al., 2014; Jiang et al., 2009; Pan et al., 2007; Park et al., 2009; Ptito et al., 2008) reported reduced gray matter volume in the occipital cortex.

Our study aimed to determine the effect of peripheral retinal loss in RP on brain function and structure using Magnetic Resonance Imaging (MRI). We studied retinotopic mapping representations and visual cortical thickness in V1 in a relatively large group of RP patients with different visual loss levels, and healthy participants with the same mean age and gender ratio. We hypothesized that V1's cortical responses change in RP as a function of the magnitude of visual loss, while brain morphology is relatively intact early on since patients are only partially deprived of visual experience. To our knowledge, this is the first study combining structural and functional brain investigations from low vision patients with the same pathology as a function of the magnitude of peripheral visual loss, thus facilitating the elucidation of possible mechanisms underlying adult brain reorganization.

2. Materials and methods

2.1. Participants

Forty-one individuals participated in this study: 14 with RP and 27 healthy or control participants. One patient and 5 control participants were excluded from our analysis. Exclusion criteria were intracranial abnormalities, movement during MRI acquisitions ($n = 1$), fixation instability ($n = 1$), or visual alterations in control subjects ($n = 3$) or visual alterations other than RP for patients (e.g. diabetic retinopathy or glaucoma, $n = 1$). Therefore, we included 13 RP individuals (8 males and 5 females; mean age 38.31 ± 12.65 years; age range 20 to 66 years; 12 right-handed and 1 left-handed; self-reported symptoms age of onset ranged from 2 to 39 years, resulting in symptoms duration range of 6 to 42 years) and 22 control subjects (11 males and 11 females; mean age 38.45 ± 12.29 years; age range 23 to 66 years; 21 right-handed and 1 left-handed). Groups were not different concerning mean age [$t_{(33)} = -0.03$, $p > 0.050$ or Non-Significant (NS)], gender ratio [$\chi^2_{(1)} = 0.44$, NS] and handedness ratio [$\chi^2_{(1)} = 0.15$, NS]. Patients were recruited in collaboration with the Ophthalmology Unit at *Centro Hospitalar e Universitário de Coimbra*, Portugal. The control group was recruited from our database of volunteers. The study was conducted in accordance with the Declaration of Helsinki and was approved by the Ethics Commission of Faculty of Medicine of the University of Coimbra. Written informed consent was obtained from all participants.

2.2. Ophthalmological assessment

For each participant, visual acuity was determined using a decimal chart and converted to logMAR scale (logarithm of Minimum Angle of Resolution) (Holladay, 1997). We used Frequency Domain Cirrus Ocular Coherence Tomography (OCT, software version 5.1.1.6, Carl Zeiss Meditec AG, USA) to measure average retinal thickness and Retinal Nerve Fiber Layer (RNFL) thickness. We acquired a macular scan with resolution 512 × 128 to assess the retinal thickness and an optic disc scan with resolution 200 × 200 to assess RNFL thickness. Static visual fields were evaluated using a MonCv3 multifunction perimeter (Metrovision, France) with a standardized program. A suprathreshold strategy was used for the 79 points tested in central 24 deg or 12 deg when patients had a narrow visual field ($n = 2$). The visual field deficit volume was automatically calculated based on sensitivity values of each visual field point and the tested visual area. The visual field diameter extent was calculated based on the results from static perimetry by excluding absolute scotoma regions (black regions with sensitivity approximately below 10 dB represented in Fig. 1). Testing was carried out with refractive correction and fixation was monitored in real time by the operator. Patients with a visual field diameter <15 deg or visual acuity <0.2 (0.70 logMAR) in both eyes were excluded due to difficulty on fixation tasks during visual examinations and fMRI acquisition. Ophthalmological examinations were evaluated by an experienced ophthalmologist (EDS) to rule out eye disorders in the control group. Table 1 summarizes the ophthalmological characterization of RP patients. Fig. 1 represents the visual field extent of the left eye (right eye scotomata were very similar) for all RP patients and 1 control participant.

2.3. Brain imaging procedures

Scanning was performed on a 3 T scanner (Magneton TrioTim, Siemens AG, Germany) at the Portuguese Brain Imaging Network, using a 12-channel birdcage head coil. Two T1-weighted Magnetization-Prepared Rapid Acquisition with Gradient Echo sequences (MPRAGE), with 1 × 1 × 1 mm^3 voxel size, Repetition Time (TR) 2.53 s, Echo Time (TE) 3.42 ms, Flip Angle (FA) 7 deg, Field Of View (FOV) 256 × 256 mm^2, and 176 slices were acquired from each participant. The functional sequence consisted in a single shot Echo Planar Imaging (EPI) acquired in the axial plane parallel to the Anterior Commissure (AC) - Posterior Commissure (PC) plane covering occipital, temporal and frontal cortices, with 2 × 2 × 2 mm^3 voxel size, TR 2 s, TE 39 ms, interslice time (TI) 76 ms, FA 90 deg, FOV 256 × 256 mm^2, 26 slices, and 128 × 128 imaging matrix.

Stimuli were monocularly presented using MRI-compatible goggles with refractive correction (VisualSystem, NordicNeurolab, Norway). One eye was covered with a cotton patch. Stimuli were presented to the dominant eye, except if it was the worst eye in terms of visual acuity to avoid higher discomfort during acquisition. Eye dominance was determined using the Dolman hole-in-the-card test. The RP and control groups were not different concerning the selected eye ratio [$\chi^2_{(1)} = 0.85$, NS] and the ratio of the dominance of the selected eye [$\chi^2_{(1)} = 0.01$, NS; 1 patient with missing data]. The maximum field of view was 23 × 30 deg, corresponding to a resolution of 600 × 800. Fixation was monitored by the operator with an eye-tracker device (EyeTracking

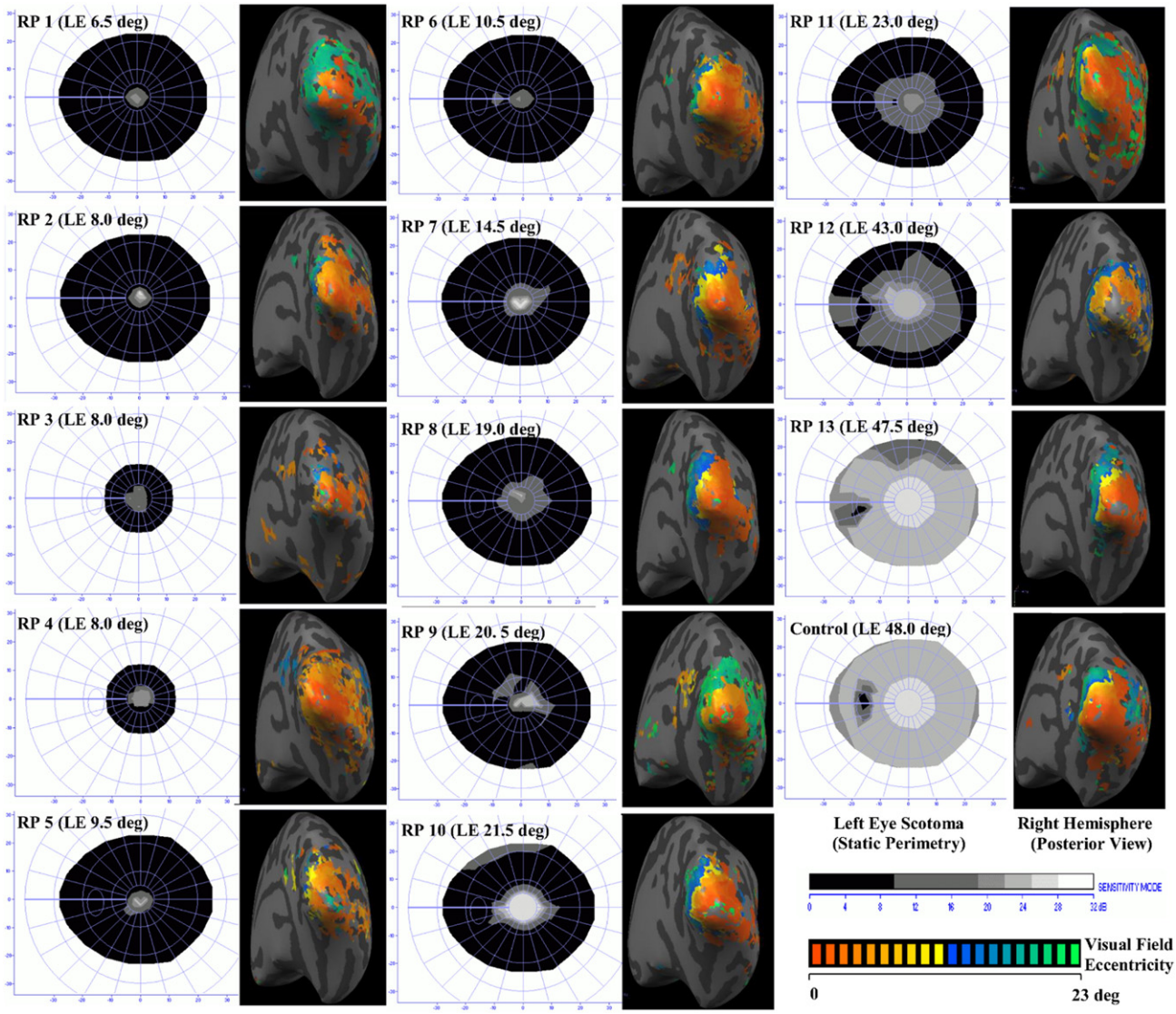

Fig. 1. Representation of the left eye lesions (scotomata) measured with static perimetry on the left side of the figure (vertical and horizontal axis represent visual field extent in degrees; the gray scale represents visual field sensitivity in dB), and right hemisphere retinotopic eccentricity maps on the right side of the figure (Linear Correlation Maps, $r > 0.25$; inflated hemisphere mesh; the color scale represents visual field eccentricity in degrees) for all patients and one control participant. Right eye scotomata and left hemisphere eccentricity maps were very similar to the ones presented, thus, their images were not displayed in this figure. RP = Retinitis Pigmentosa, LE = Left Eye.

Camera, NordicNeurolab, Norway). All anatomical images were evaluated by a neuroradiologist to exclude clinical alterations.

2.4. MRI stimuli and experimental design

Stimuli were designed using Matlab 2011b (The MathWorks, Inc., USA) with Psychophysics Toolbox 3 extensions (http://psychtoolbox.org/). A central red-colored cross with 0.78 deg of diameter was used for fixation and no task was required from participants.

Eccentricity maps were obtained using a black and white flickering checkerboard expanding ring from the standard phase-encoded retinotopic mapping (Wandell et al., 2007). Checkerboard ring size varied with cortical magnification factor from center to periphery (Duncan and Boynton, 2003; Strasburger et al., 2011). Stimuli flickering frequency was 8 Hz and contrast was ~100%. Each run comprised 2 baseline blocks (~0% contrast; 12 s) at beginning and end of the run with 4 cycles of eccentricity stimuli (48 s each; total duration of a run 216 s). During each cycle of eccentricity stimuli, the ring size increased continuously from the center to the periphery. Two runs of eccentricity were acquired for each subject.

2.5. Structural and functional MRI data processing

Brain imaging analysis was carried out using BrainVoyager QX 2.6.1 (Brain Innovation B. V., The Netherlands). The 2 high-resolution anatomical images were averaged to improve the signal-to-noise ratio. Anatomical volumes were re-oriented in relation to AC–PC plane and transformed to Talairach (TAL) coordinate system. Afterwards, the cerebral cortex was segmented into the cerebral spinal fluid, gray matter, and white matter using automatic segmentation routines in order to create inflated mesh representations of each hemisphere (d'Almeida et al., 2013).

Scan time correction, temporal high-pass filtering (2 cycles per run), spatial smoothing (FWHM 2 mm), and a correction for small interscan head movements were applied during functional image preprocessing. Participants were excluded from further analysis if any within-run movement exceeded ± 2 mm. Eccentricity maps were obtained from

Table 1
Summary of the participants' characterization and ophthalmological tests results for the Retinitis Pigmentosa group.

Patient	Age (years)	Gender	Handedness	Onset age (years)	Disease duration (years)	Visual acuity (decimal/logMAR)		Retinal thickness (μm)		RNFL thickness (μm)		Visual Field deficit volume (dB.deg^2)		Visual field extent (~ diameter in deg)	
						LE	RE	LE	RE	LE	RE	LE	RE	LE	RE
RP 1	66	F	R	27	39	0.50/0.30	0.50/0.30	254.00	248.00	95.00	108.00	1349.00	1349.00	6.50	6.50
RP 2	42	M	R	18	24	0.60/0.22	0.50/0.30	194.00	208.00	100.00	116.00	1718.00	1757.00	8.00	4.50
RP 3	50	M	R	16	34	0.50/0.30	0.50/0.30	201.00	203.00	70.00	62.00	1168.00	1156.00	8.00	8.00
RP 4	23	M	R	16	7	0.50/0.30	0.66/0.18	254.00	266.00	130.00	143.00	1240.00	1232.00	8.00	8.50
RP 5	35	M	R	6	29	0.90/0.05	0.50/0.30	228.00	243.00	89.00	91.00	1700.00	1700.00	9.50	10.50
RP 6	45	F	R	39	6	0.80/0.10	0.66/0.18	192.00	184.00	76.00	81.00	1204.00	1181.00	10.50	8.50
RP 7	20	M	R	7	13	0.60/0.22	0.60/0.22	225.00	228.00	106.00	99.00	1639.00	1666.00	14.50	13.00
RP 8	35	F	R	3	32	0.30/0.52	0.60/0.22	281.00	265.00	101.00	101.00	1650.00	1609.00	19.00	15.50
RP 9	50	M	L	8	42	0.66/0.18	0.40/0.40	205.00	207.00	79.00	73.00	1414.00	1402.00	20.50	18.50
RP 10	38	F	R	32	6	1.00/0.00	0.40/0.40	249.00	258.00	128.00	128.00	1520.00	1423.00	21.50	21.00
RP 11	38	F	R	6	32	0.80/0.10	0.28/0.55	216.00	221.00	133.00	109.00	1118.00	1030.00	23.00	29.00
RP 12	25	M	R	14	11	0.40/0.40	0.50/0.30	242.00	245.00	101.00	95.00	802.00	539.00	43.00	43.00
RP 13	31	M	R	2	29	0.80/0.10	0.40/0.40	273.00	268.00	91.00	92.00	72.00	126.00	47.50	47.00

RP = Retinitis Pigmentosa; F = Female; M = Male; R = Right hand; L = Left hand; LE = Left eye; RE = Right eye; RNFL = Retinal nerve fiber layer; logMAR = Logarithm of minimum angle of resolution.

the average of the 2 runs, created based on linear regression analysis and projected onto the inflated surfaces of each subject. Voxels were included into the statistical map if $r > 0.25$. Fig. 1 represents the eccentricity maps only for the right hemisphere for all patients and 1 control participant (the maps on left hemisphere had a similar pattern).

We used an individual General Linear Model (GLM) [*z*-transformation, correction for temporal serial correlations AR(2), predictors for within-run movements, and $p < 0.05$] by defining 8 predictors for the response to the expanding ring in the eccentricity stimulus (8 rings with different eccentricity positions or diameters: $0.78 \leq Ring_1 \leq 3.65$, $3.65 < Ring_2 \leq 6.53$, $6.53 < Ring_3 \leq 9.40$, $9.40 < Ring_4 \leq 12.28$, $12.28 < Ring_5 \leq 15.15$, $15.15 < Ring_6 \leq 18.03$, $18.0 < Ring_7 \leq 20.90$, and $20.90 < Ring_8 \leq 23.00$ deg). The activation elicited by each eccentricity ring was projected on the inflated meshes. The most anterior point of the cortical representation of each ring along the calcarine sulcus in V1 was recorded and then the distance between this point and the occipital pole was calculated for each participant. The calcarine sulcus has a more accurate retinotopic representation of the transition from central to the peripheral visual field (see Fig. 1) and contains part of V1. The occipital pole was defined as the center of the cortical activation for $Ring_1$ for each participant. For some RP participants, the cortical representations of more peripheral rings were absent [$Ring_5$ Left Hemisphere (LH) ($n = 3$), $Ring_5$ Right Hemisphere (RH) ($n = 1$), $Ring_6$ LH ($n = 2$), $Ring_6$ RH ($n = 1$), $Ring_7$ LH ($n = 3$), $Ring_8$ LH ($n = 1$), $Ring_8$ RH ($n = 1$)]. These absent or reduced responses may be explained by the limited or damaged peripheral visual field in these patients since they have a visual field diameter under 15 deg Fig. 2 illustrates the eccentricity position of the rings on the visual field and the cortical representation of the rings on the right hemisphere for the RP and control groups, as well as the difference in activation between groups. The length of the calcarine sulcus was also manually measured on the mesh of both hemispheres based on anatomical landmarks, starting at the occipital pole and ending below the isthmus of cingulate gyrus (Klein and Tourville, 2012). The calcarine sulcus length was used to account for V1 size variability among individuals.

We defined 2 different cortical regions of interest in the calcarine zone to determine the cortical thickness of V1: the Lesion Projection Zone (LPZ) representing the calcarine region with no cortical response to the eccentricity stimulus, and the Function Projection Zone (FPZ) representing the calcarine responsive region (based on the eccentricity maps shown in Fig. 1). In this way, the LPZ corresponds to the retinal scotomata in RP patients and the FPZ corresponds to the spared retina. Cortical thickness was calculated on the V1 regions using the standard procedure of BrainVoyager [see (d'Almeida et al., 2013) for a complete description]. To allow an accurate segmentation of white matter–gray matter and gray matter–cerebral spinal fluid boundary, TAL anatomical data were converted to high-resolution $0.5 \times 0.5 \times 0.5$ mm^3. The subcortical structures and the ventricles were filled as white-matter. After computation, cortical thickness maps were superimposed on cortical meshes and the mean cortical thickness values of the visual regions of interest were extracted using Matlab BVQXtools toolbox extensions (http://support.brainvoyager.com/available-tools/52-matlab-tools-bvxqtools.html). The average cortical thickness of each hemisphere was also determined to account for variability among individuals.

2.6. Statistical analysis

Statistical analysis was performed with IBM SPSS Statistics, Version 22 (IBM Corporation, USA). First, normality assumptions for all variables were tested using the Shapiro Wilk's test. For data in accordance with the assumptions, statistical parametric tests were performed (independent-samples *t*-test [*t* parameter] and Analysis of variance (ANOVA) [*F* parameter]). Otherwise, non-parametric methods were applied (Mann-Whitney [*U* parameter], Wilcoxon Signed-Rank [*Z* parameter], Kruskal-Wallis [χ^2 parameter, differences between group], and Friedman tests [χ^2 parameter, differences within group], and Linear Mixed Models [*F* parameter]).

3. Results

3.1. Visual examinations

Visual acuity [Left Eye (LE) $U = 11.00$, $p = 2.642 \times 10^{-7}$ and Right Eye (RE) $U = 0.00$, $p = 1.355 \times 10^{-9}$] and average retinal thickness [LE $U = 275.00$, $p = 1.883 \times 10^{-7}$ and RE $U = 283.00$, $p = 9.483 \times 10^{-9}$] were reduced in both eyes for patients as compared to control participants. Visual field deficit volume [LE $U = 3.00$, $p = 9.483 \times 10^{-9}$ and RE $U = 2.00$, $p = 5.419 \times 10^{-9}$] was higher in both eyes for patients as compared to the control group. No differences were found for RNFL thickness in both eyes between the two groups [LE $U = 125.00$, NS and RE $U = 120.00$, NS]. Moreover, no statistically significant differences were found between the left and right eyes within groups for visual acuity [RP $Z = -1.33$, NS and Control $Z = -1.41$, NS], average retinal thickness [RP $Z = -0.84$, NS and Control $Z = -0.88$, NS], RNFL thickness [RP $Z = 0.00$, NS and Control $Z = -0.07$, NS], visual field deficit volume [RP $Z = -1.24$,NS and õControl $Z = -0.28$, NS], and visual field extent [RP $Z = -1.18$, NS; controls have a constant visual field extent equal to 48 deg corresponding to the maximum diameter covered by static perimetry]. Table 2 shows a summary of participants' ophthalmologic characterization.

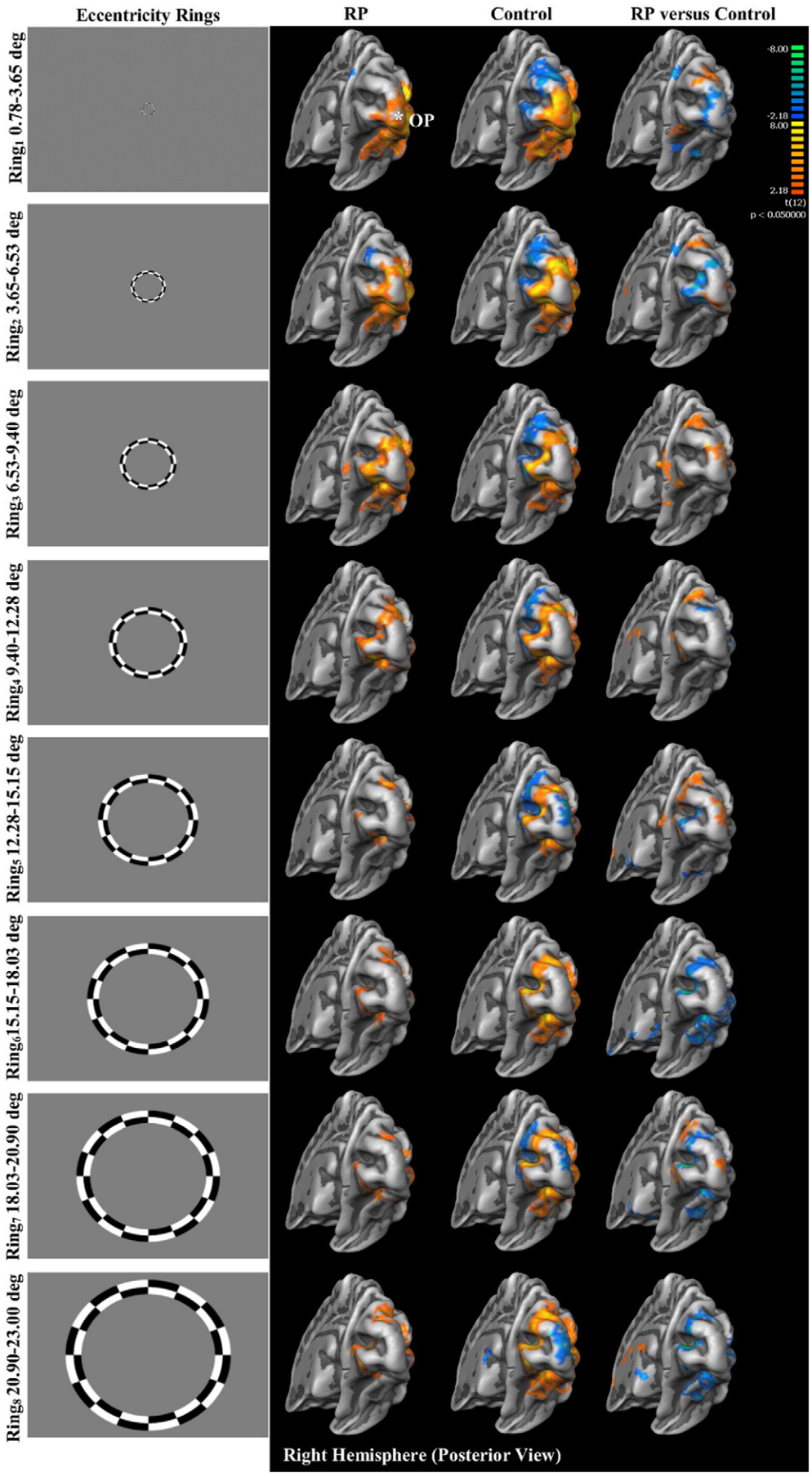
Eccentricity Rings
RP
Control
RP versus Control
Ring1 0.78-3.65 deg
Ring2 3.65-6.53 deg
Ring3 6.53-9.40 deg
Ring4 9.40-12.28 deg
Ring5 12.28-15.15 deg
Ring6 15.15-18.03 deg
Ring7 18.03-20.90 deg
Ring8 20.90-23.00 deg
* OP
-8.00
-2.18
8.00
2.18
t(12)
p < 0.050000
Right Hemisphere (Posterior View)

Ophthalmological examinations yielded a severe decrease of patients' visual function concerning visual acuity, visual field extent and average retinal thickness, consistent with the loss of photoreceptors in the retina (Bittner et al., 2011; Hamel, 2006; Hartong et al., 2006; Jacobson et al., 2010; Rangaswamy et al., 2010; Shintani et al., 2009; Van Soest et al., 1999). RNFL thickness was unchanged and this result is supported by previous works reporting thinning, thickening, or maintenance of RNFL in RP patients which is probably related to the level of peripheral degeneration (Oishi et al., 2013, 2009; Walia et al., 2007; Walia and Fishman, 2008). It is worth mentioning that two patients presented retinal edema (RP 9 and RP 12), which may lead to an overestimation of the retinal and RNFL thickness.

3.2. Eccentricity rings

No differences were found between the length of the calcarine sulcus between the studied RP and control groups [$F_{(1,33)} = 4.50 \times 10^{-5}$, NS], and there were no differences within-groups between the left and the right hemispheres [$F_{(1,33)} = 1.16$, NS]. Therefore, the length of calcarine sulcus of each hemisphere was used to normalize the cortical distance for the eccentricity rings to account for variability among individuals. The ratio between the rings' cortical distance and the length of calcarine sulcus of each hemisphere was used in the further analysis.

Group differences in rings' cortical distance to the occipital pole were investigated using Linear Mixed Models due to unequal variances between groups and missing data for the RP group [$Ring_5$ LH ($n = 3$), $Ring_5$ RH ($n = 1$), $Ring_6$ LH ($n = 2$), $Ring_6$ RH ($n = 1$), $Ring_7$ LH ($n = 3$), $Ring_8$ LH ($n = 1$), $Ring_8$ RH ($n = 1$)] (Cnaan et al., 1997). The repeated measures factors used were *Ring* (1–8) and *Hemisphere* (LH vs RH), and the between-subject factors were *Group* (RP vs Control) and *Hemisphere* (LH vs RH). The fixed effect interactions tested were *Group* (RP vs Control) and *Hemisphere* × *Group*. The covariance structure for the random effects model was Identity, and random effects interactions were considered for each participant in the sample. The Restricted Maximum Likelihood method was chosen for the model. We found statistically significant fixed effects of *Group* [$F_{(1,32.09)} = 5.63$, $p = 0.024$] and *Hemisphere* × *Group* [$F_{(2,347.21)} = 8.90$, $p = 1.700 \times 10^{-4}$]. The distances of rings' representation to the occipital pole were greater for RP patients than for the control group. Additionally, the RP group had larger cortical distances in the left hemisphere when compared to the right hemisphere [$t_{(358.78)} = 4.17$, $p = 3.800 \times 10^{-5}$], in contrast to the control group where no differences were found between the two hemispheres [$t_{(336.36)} = 4.17$, NS]. Fig. 3 illustrates the increased cortical distance of both hemispheres in RP group for all eccentricity rings when compared to controls.

An additional analysis was conducted to test if patients with more severe visual loss levels presented more pronounced cortical remapping with increased cortical distances for eccentricity rings in V1. In this way, we divided the RP group into two subgroups depending on the visual field extent: RP A (patients RP 1 to RP 7) with <15 deg of visual field diameter and RP B (patients RP 8 to RP 13) with >15 deg of visual field diameter in both eyes, and applied a Linear Mixed Model [repeated measures factor *Ring* (1–8) and *Hemisphere* (LH vs RH), and between-subject factors *Group* (RP A, RP B, and Control) and *Hemisphere* × *Group*]. The logic underlying the division is as follows: the RP group was divided in the RP A subgroup with remaining foveal and parafoveal vision, this is, with total loss of peripheral vision and partial macular visual loss (below 15 degrees of visual field), and the RP B subgroup with partial peripheral visual loss (above 15 degrees of visual field) (Strasburger et al., 2011). Results showed statistically significant fixed effects of *Group* [$F_{(2,31.01)} = 5.33$, $p = 0.010$] and *Hemisphere* × *Group* [$F_{(3,336.18)} = 8.93$, $p = 1.000 \times 10^{-5}$]. RP A patients with lower visual field extents presented increased cortical distance when compared to RP B and control groups [$t_{(34.91)} = 2.09$, $p = 0.044$]. Additionally, the RP A subgroup had larger cortical distances in the left hemisphere when compared to the right hemisphere [$t_{(368.78)} = 4.91$, $p = 1.000 \times 10^{-6}$], in contrast to the RP B [$t_{(321.96)} = 1.45$, NS] and control groups [$t_{(321.96)} = 0.75$, NS] where no differences were found between the two hemispheres. Fig. 3 also illustrates the increased cortical distance in subgroup RP A as compared to subgroup RP B and the control group in both hemispheres.

We also used Spearman's correlations to investigate the correlation between RP disease duration and visual field extent, and also between the disease onset age and visual field extent. No correlations were found for the disease duration or the disease onset age in the RP group including all patients [$p \geq 0.054$], and for the two RP subgroups [$p \geq 0.337$]. In this way, we do not expect that the increased cortical distance found in RP patients and RP A patients is associated with disease onset age or disease duration, but rather more directly with the extent of changes in visual experience.

3.3. Cortical thickness

The average cortical thickness of left [$U = 95.00$, NS] and right [$U = 90.00$, NS] hemispheres was not different between groups and there was no within-subject effect of the hemisphere for RP [$Z = -0.80$, NS] and control [$Z = -1.05$, NS] groups. The primary visual cortical thickness (V1) was normalized with the average cortical thickness of the respective hemisphere to account for variability across individuals. The ratio between V1 cortical thickness and the average cortical thickness of each hemisphere was used in the subsequent analysis.

Visual cortical thickness differences in the two V1 regions (FPZ and LPZ) for each hemisphere were evaluated using the Mann-Whitney or Kruskal-Wallis test for between-subject's effects and the Friedman test for within-subject's effects considering the hemisphere and the V1 region as factors. Cortical thickness of V1 was not different between the RP and control groups [$U \geq 101.00$, $p \geq 0.159$] for both V1 regions in both hemispheres. Additionally, no differences were found between the thickness of the V1 regions for each hemisphere within-groups, and no differences were found for the same V1 region between hemispheres within-groups [$\chi^2_{(3)} \leq 7.80$, $p \geq 0.050$].

The analysis described above was repeated for the two subgroups of patients, RP A with <15 deg of visual field diameter and RP B with >15 deg of visual field diameter, and the control group, to test for V1 changes in terms of cortical thickness. Cortical thickness of the V1 FPZ in the left hemisphere was different among the three groups [$\chi^2_{(2)} = 10.65$, $p = 0.005$], with RP A patients presenting higher cortical thickness than RP B patients [$t = 3.25$, $p = 0.003$ with Bonferroni correction for multiple comparisons]. However, the left FPZ V1 cortical thickness of both subgroups of patients was not different from the control group [$t = 1.67$, NS for RP A and $t = -2.35$, NS for RP B, with Bonferroni correction for multiple comparisons]. Additionally, no differences were found between the thickness of the V1 regions for each hemisphere within the RP A and the control groups [$\chi^2_{(3)} \leq 7.80$, $p \geq 0.050$]. For the RP B patients, we found that the thickness of the FPZ in the left hemisphere was decreased in comparison to the right FPZ [$t = -2.00$, $p = 0.044$, with Bonferroni correction for multiple comparisons]. Fig. 4 represents the normalized cortical thickness in the FPZ and LPZ V1 regions in both hemispheres for all the studied groups.

4. Discussion

We acquired brain data with MRI from thirteen RP patients with peripheral retinal degeneration and twenty-two healthy participants to

Fig. 2. Representation of the eight eccentricity rings stimuli in the visual field and their respective cortical representation in the right hemisphere (multi-study General Linear Model, $p < 0.050$; average group mesh). Cortical responses for Retinitis Pigmentosa and control groups are shown for each eccentricity ring, as well as the response contrast between the two groups. The color bar represents the *t*-values from the General Linear Model. RP = Retinitis Pigmentosa; OP = Occipital Pole.

Table 2
Ophthalmological characterization of the participants from the patients' and controls' groups and the Mann-Whitney test results for comparisons between the two groups. No statistically significant differences were found between the left and right eyes within groups for all visual parameters displayed in the table (Wilcoxon Signed-Rank test).

Visual parameters	Eye	RP group ($n = 13$)	Control group ($n = 22$)	Mann-Whitney test	
				U value	*P* value
Visual acuity (decimal/logMAR)	LE	0.60 (0.30)/0.22 (0.20)	1.00 (0.30)/0.00 (0.11)	11.00	2.64×10^{-7}
	RE	0.50 (0.20)/0.30 (0.18)	1.00 (0.30)/0.00 (0.11)	0.00	1.35×10^{-9}
Retinal thickness (μm)	LE	228.00 (51.00)	288.50 (21.50)	275.50	1.88×10^{-7}
	RE	243.00 (54.00)	285.00 (20.75)	283.00	9.48×10^{-9}
RNFL thickness (μm)	LE	100.00 (33.00)	94.50 (10.50)	125.00	Non-significant
	RE	99.00 (26.50)	95.00 (17.25)	120.00	Non-significant
Deficit volume of Visual field ($dB.deg^2$)	LE	1349.00 (401.50)	30.00 (24.25)	3.00	9.48×10^{-9}
	RE	1349.00 (544.50)	27.50 (44.00)	2.00	5.42×10^{-9}
Visual field extent (~diameter; deg)	LE	14.50 (14.25)	48[a]	–	–
	RE	13.00 (16.75)	48[a]	–	–

Data are median (interquartile range); RP = Retinitis Pigmentosa; LE = Left Eye; RE = Right Eye; RNFL = Retinal Nerve Fiber Layer; logMAR = Logarithm of Minimum Angle of Resolution.
[a] Visual field extent for the control group is the maximum diameter tested during the static perimetry (48 deg).

investigate structural changes and functional remapping of primary visual cortex (V1) as a function of visual impairment. Results seem to indicate a topographic remapping of visual field eccentricity in V1 in the patient group, with a shift of central retinal representations to more peripheral locations. This remapping was associated with the magnitude of visual loss extent, with more constricted visual fields linked to a larger remapping. Importantly, no gray matter thickness alterations were found in RP patients' V1 when compared to controls. Nonetheless, RP patients with more severe visual field degeneration (RP A) presented higher cortical thickness in the central regions of V1 representing the spared retina (FPZ) when compared to patients with larger visual field extent (RP B).

Our data suggests that retinal projections seem to be represented more peripherally in V1 in the patients' group. V1 cortical remapping of the visual input was more evident for patients with a visual field diameter lower than 15 deg (RP A), while patients with higher visual extent (RP B) had topographical representations more similar to controls (see Fig. 3), suggesting dependence on the level of change in visual experience. In this way, our results suggest that cortical remapping in V1 may occur at a larger scale when patients have lost their peripheral visual fields, that is, when only central and paracentral vision is spared. An analogous hypothesis was proposed in macular degeneration studies where authors claimed that large-scale remapping of central cortical representations only occurs when patients have completely lost their foveal vision (Baker et al., 2008; Dilks et al., 2014). Cortical remapping observed in the RP group may not be influenced by disease duration or onset age, in contrast to the extent of the visual loss, since no correlations were found between age of onset and visual field extent or disease duration and visual field extent. This may be due to the fact that disease age of onset as documented in the clinical history is a relatively imprecise measure of RP severity (Hamel, 2006; Hartong et al., 2006). Importantly, our eccentricity stimulus only covered a part of the peripheral visual field (23 deg of diameter) preventing the investigation of putative cortical remapping in more peripheral eccentricities in patients with larger visual field extents. Remaining peripheral islands of vision in some patients might also influence the differences among the studied groups. Additionally, cortical responses resulting from the more peripheral rings seem to be reduced (see Fig. 2), suggesting weaker responses in RP patients. Moreover, some patients from the RP A subgroup with smaller visual field extent had no identifiable representations in the calcarine sulcus of the more peripheral rings.

RP patients presented a hemispheric difference regarding the distances of the eccentricity rings, in contrast to the control participants. We are unable to explain why RP patients had larger cortical distances in the left hemisphere when compared to the right hemisphere. Moreover, previous studies with retinal disorders largely used average data from the two hemispheres, masking possible hemispheric differences. This results may indicate that the left visual cortex has larger remapping than the right hemisphere in patients with more severe visual loss, since this result was found to stem from the RP A subgroup.

Our results differ to some extent from the previous studies (Goesaert et al., 2014; Masuda et al., 2010) with RP patients where authors found evidence of a conspicuous silent cortical zone matching patients' scotomata under passive viewing stimulation, consistent with the idea that remapping does not necessarily occur. However, the patients' visual field extent in that studies was larger than in our RP A group, ranging

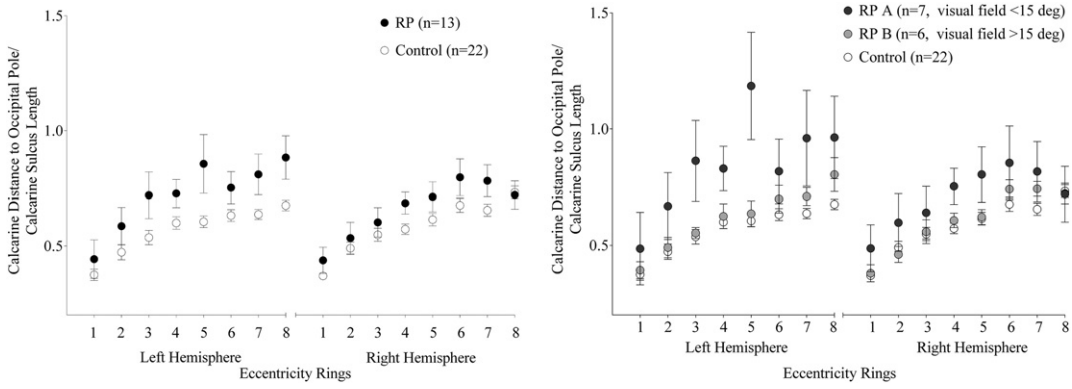

Fig. 3. Ratio between the cortical distance to the occipital pole of the eight eccentricity rings' representation along the calcarine sulcus and the length of calcarine sulcus for patients' and controls' groups in both hemispheres (in left side of the figure). The distances were higher for the Retinitis Pigmentosa group as compared to control participants (Linear Mixed Model, $F_{(1,32.09)} = 5.63$, $p = 0.024$). The right side of the figure represents the same distance for RP A (with <15 deg of visual field diameter) and RP B (with >15 deg of visual field diameter) patients' subgroups and the control group, with augmented distances for subgroup RP A (Linear Mixed Model, $F_{(2,31.01)} = 5.33$, $p = 0.010$) when compared to RP B patients and the control group. Error bars represent data standard error. RP = Retinitis Pigmentosa.

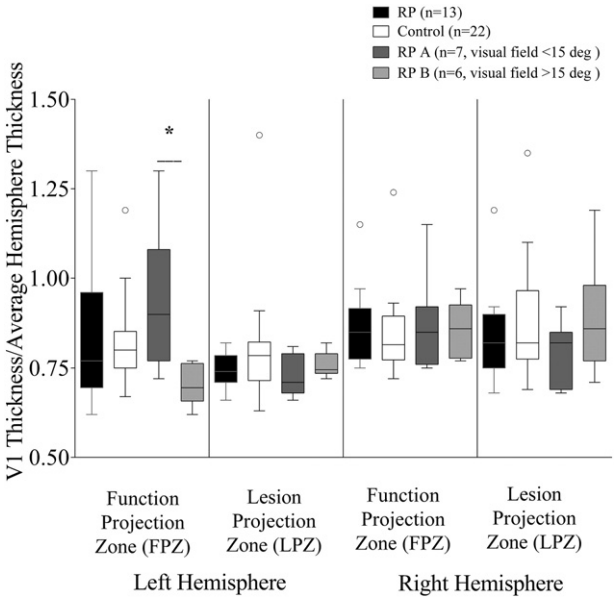

Fig. 4. Ratio between primary visual cortical thickness and the average hemisphere thickness for the Lesion Projection Zone (LPZ) and Function Projection Zone (FPZ) regions in the calcarine sulcus for patients' and controls' groups in both hemispheres. RP A patients (with <15 deg of visual field diameter) presented augmented left cortical thickness in the FPZ in comparison to RP B patients (with >15 deg of visual field diameter) [*statistical significance with $t = 3.25$ and $p = 0.003$]. RP = Retinitis Pigmentosa.

from 10 to16 deg, thus, cortical maps may have been more similar to the control participants because central vision was barely affected.

The cortical modifications reported here may differ from the alterations in V1 cortical responses in relation to peripheral visual loss reported in glaucoma studies (Dai et al., 2012; Duncan et al., 2007a, 2007b; Engin et al., 2014; Lešťák and Tintěra, 2011; Qing et al., 2010). In glaucoma, retinal ganglion cell death affects the entire visual pathway through transsynaptic degeneration (Engelhorn et al., 2011; Engin et al., 2014; Gupta et al., 2009). Here, we found no evidence of RNFL degeneration, suggesting that retinal ganglion cells might be preserved in the RP group. Furthermore, V1 structure in the cortical region deprived of retinal input (LPZ) was preserved even in patients with more severe visual loss.

Regarding central visual loss, many authors have found unresponsive cortical zones representing the damaged central retina in macular degeneration (Baseler et al., 2011a, 2011b; Lešťák et al., 2013; Liu et al., 2010; Masuda et al., 2008; Sunness et al., 2004). Cortical regions representing the uninjured peripheral visual field may be insufficient to trigger activation in a large number of deprived neurons since central vision is represented in a larger extent of V1. Differences in connections with higher order and subcortical areas between central and peripheral visual neurons may also account for a distinct probability of remapping (Butz and van Ooyen, 2013; Hernowo et al., 2014; Ruff et al., 2008; Smirnakis et al., 2005; Visscher et al., 2014; Vossel et al., 2014; Wandell et al., 2007; Wang and Yamamoto, 2013). Hernowo et al. (2014) found conspicuous visual pathway degeneration similar to glaucoma in a large group of macular degeneration patients, which may explain the lack of functional reorganization in the studies mentioned above. Retinal ganglion cells might also degenerate in macular degeneration leading to visual cortical atrophy and diminishing the probability of functional remapping. However, other authors (Baker et al., 2008; Dilks et al., 2009; Schumacher et al., 2008) found cortical reorganization in macular degeneration when stimulating the peripheral retina. Reduced numbers of participants (Baseler et al., 2011a; Sunness et al., 2004), different levels of foveal vision (Baseler et al., 2011a; Lešťák et al., 2013; Masuda et al., 2008; Schumacher et al., 2008; Sunness et al., 2004), distinct disease mechanisms - juvenile and age-related macular degeneration (Baseler et al., 2011b; Liu et al., 2010; Schumacher et al., 2008), age differences between studied groups (Crossland et al., 2008; D'Esposito et al., 2003; Lešťák et al., 2013; Masuda et al., 2008), and the use of complex stimuli involving higher level areas (Liu et al., 2010) may also contribute to the controversy arising from the interpretation of results from macular degeneration studies (Baseler et al., 2009; Martins Rosa et al., 2013).

Our findings are consistent with the idea that neurons representing the remaining visual field may exert influence onto the partially deprived visual cortex in the RP group. The axonal sprouting and strengthening of long-range horizontal connections within V1 may lead to expansion and/or shifting of neuronal receptive fields into the cortical regions with altered retinal input. The inhibitory neuronal inputs inside the deprived visual cortex may be weakened, leading to an increase of excitatory horizontal connections with neurons in regions adjacent to the deprived region (Botelho et al., 2014; Butz and van Ooyen, 2013; Darian-Smith and Gilbert, 1995; Engel et al., 2015; Giannikopoulos and Eysel, 2006; Gilbert and Li, 2012; Marik et al., 2014; Pascual-Leone et al., 2005; Sammons and Keck, 2015; Shao et al., 2013; Wandell and Smirnakis, 2009; Yamahachi et al., 2009). Some authors have suggested the use of an artificial scotoma to mimic the patients' visual field extent, to help elucidate the origin of remapping (Goesaert et al., 2014; Masuda et al., 2010). Previous works applying central artificial scotomata in healthy participants (Barton and Brewer, 2015; Baseler et al., 2011b; Haak et al., 2012) reported a visual cortical remapping similar to the effects usually seen in patients. Given that we did not use this approach, two possible explanations remain possible to explain functional remapping in our group of patients: fast adaptation or long term reorganization mechanisms. It is possible that these visual cortical functional alterations may indeed result from a fast acting mechanism rather than a long-term reorganization process (Wandell and Smirnakis, 2009). Future experiments with healthy participants with an artificial scotoma representing the visual field limitations of RP patients may help clarify the mechanism that underlies the V1 cortical remapping reported here. Moreover, longitudinal studies to analyze the long-term effects of peripheral retinal degeneration on visual cortex may also be important to clarify this mechanism (Lemos et al., 2016; Prins et al., 2016a).

Importantly, our results did not show evidence for V1 structural alterations in RP patients when compared to the control group. Even so, our results point to an increase in V1 thickness in the left hemisphere for the central region representing the spared visual field (FPZ) but only when comparing RP A and RP B patients. This difference was not significant in relation to the control group. Accordingly, the central portion of V1 might have increased gray matter thickness to compensate the loss of retinal input from the most peripheral V1 regions in the more advanced stages of the disease. Nonetheless, structural atrophy may exist in higher-order visual areas beyond V1 which we did not take into account in this study.

Few structural MRI studies have been conducted with low vision RP patients (Prins et al., 2016a). Furthermore, a diffusion tensor imaging study with five late-blind RP patients reported no difference in the fractional anisotropy of the visual fiber tracts, supporting the preservation of the visual pathway suggested by our results (Schoth et al., 2006). Moreover, a recent study comparing two blind RP patients implanted with a retinal prosthesis, nine non-implanted RP patients (low vision and blind), and nine controls did not find structural differences among all groups concerning V1 cortical thickness and the diffusion properties of the optic tract and optic radiation (Cunningham et al., 2015). Their results are also in accordance with our work supporting the preservation of the visuo-cortical pathways in RP. Additionally, a recent study with macular degeneration patients found increased thickness in the peripheral regions of V1 when central vision degenerates, which also supports the increased cortical thickness in the left central FPZ in RP A patients

with more severe peripheral visual loss (Burge et al., 2016). They suggested that macular degeneration patients rely more on peripheral vision to compensate the central visual loss.

Previous studies with low vision patients with glaucoma and macular degeneration reported reduced gray matter volume in occipital cortex consistent with the visual field scotomata (Bogorodzki et al., 2014; Boucard et al., 2009; Burge et al., 2016; Chen et al., 2013; Gupta et al., 2006; Hernowo et al., 2014; Kitajima et al., 1997; Kitsos et al., 2009; Olivo et al., 2015; Plank et al., 2011; Prins et al., 2016a, 2016b, Yu et al., 2014, 2013; Zikou et al., 2012). Retinal ganglion cell degeneration in glaucoma, and also in macular degeneration after photoreceptors death, may cause transneuronal degeneration along visuo-cortical pathways, leading to neuronal atrophy in visual cortex. RP patients did not present RNFL thickness atrophy which is in line with the preservation of visual cortical thickness. Studies with early and late blind individuals have also provided evidence for gray matter volume reduction in visual cortex. In late blind individuals, visual cortex seems to present reduced surface area and unchanged or reduced cortical thickness due to disuse-driven mechanisms associated with changes in synaptic density, dendritic spine numbers and axonal arborization (Anurova et al., 2014; Jiang et al., 2009; Noppeney et al., 2005; Pan et al., 2007; Park et al., 2009; Ptito et al., 2008).

In our case, the functional remapping found in the primary visual cortex of the RP group may have delayed the cortical degeneration effect of disuse-driven mechanisms in V1, preventing occipital cortical atrophy, or even leading to an increase in cortical thickness in FPZ for more severe visual loss cases. Indeed, the major functional and structural alterations in our study were found in left V1 for the RP A subgroup, the one with the most severe visual loss. In more advanced stages of RP disease with higher photoreceptor and retinal ganglion cells loss, disuse-driven mechanisms may overlap with functional processes, leading to the visual cortical atrophy pattern that is often seen in macular degeneration, glaucoma, and late-blindness.

4.1. Study limitations

Patients demonstrated good fixation capacity inside the scanner when monitored with the eye-tracker camera but we cannot exclude that minor fixation instabilities might have added noise to the signal, although not having a major influence on activity pattern changes (Bressler and Silver, 2010; Crossland et al., 2008). Although the sample is larger than other studies in the literature (Goesaert et al., 2014; Masuda et al., 2010), the heterogeneity among patients should nevertheless be considered. RP is a rare disease and a few preselected patients were excluded because they had severe visual impairment, being unable to perform the required tasks. Our results support the need for future longitudinal studies with larger sample sizes and different disease stages in order to more clearly understand the impact of long-term peripheral retinal degeneration on visual cortical remapping (Lemos et al., 2016; Prins et al., 2016a).

5. Conclusions

We identified retinotopic remapping in the absence of structural changes in primary visual cortex of patients with peripheral retinal degeneration. Remapping consisted in a retinotopic eccentricity shift of central retinal inputs to more peripheral locations in primary visual cortex and was associated with the extent of the visual loss, with more constricted visual fields resulting in larger remapping. It is possible that axonal sprouting and strengthening of long-range horizontal connections within primary visual cortex may lead to expansion and/or shifting of neuronal receptive fields into the cortical regions with altered retinal input, leading to cortical functional remapping. Future studies could clarify these mechanisms by using an artificial scotoma simulating the patients' visual field. In this way, we might be able to understand if short-term mechanisms might be sufficient to generate these changes instead of cortical reorganization mechanisms. Additionally, longitudinal studies to analyze the long-term effects of peripheral retinal degeneration on visual cortex are also warranted.

This study highlights the importance of analyzing the retinal determinants of brain functional and structural alterations to better understand plasticity mechanisms of visual cortex and future visual restoration approaches.

Conflict of interest

The authors declare that there is no conflict of interest regarding the publication of this paper.

Acknowledgements

We would like to thank Carlos Ferreira, João Marques and Sónia Afonso for technical assistance in the magnetic resonance acquisitions and the *Association for Innovation and Biomedical Research on Light and Image* (AIBILI, http://www.aibili.pt/) for cooperation with ophthalmological examinations. We also thank Dorothy Poggel for the permission to assess unpublished results (Poggel et al., 2007, n.d.). We express our sincere thanks to the patients and their families as well as other participants for their precious collaboration. This work was supported by the Portuguese *Funding Agency Foundation for Science and Technology* (FCT) [E-Rare2-SAU/0001/2008, E-Rare4/0001/2012 and FCT-UID/4539/2013 – COMPETE, POCI-01-0145-FEDER-007440].

References

Anurova, I., Renier, L.A., De Volder, A.G., Carlson, S., Rauschecker, J.P., 2014. Relationship between cortical thickness and functional activation in the early blind. Cereb. Cortex [Epub ahead of print]. 10.1093/cercor/bhu009.

Baker, C., Dilks, D., Peli, E., Kanwisher, N., 2008. Reorganization of visual processing in macular degeneration: replication and clues about the role of foveal loss. Vis. Res. 48:1910–1919. http://dx.doi.org/10.1016/j.visres.2008.05.020.

Barton, B., Brewer, A.A., 2015. fMRI of the rod scotoma elucidates cortical rod pathways and implications for lesion measurements. Proc. Natl. Acad. Sci. U.S.A. 112: 5201–5206. http://dx.doi.org/10.1073/pnas.1423673112.

Baseler, H.A., Gouws, A., Morland, A.B., 2009. The organization of the visual cortex in patients with scotomata resulting from lesions of the central retina. Neuro-Ophthalmology 33:149–157. http://dx.doi.org/10.1080/01658100903050053.

Baseler, H.A., Gouws, A., Crossland, M.D., Leung, C., Tufail, A., Rubin, G.S., Morland, A.B., 2011a. Objective visual assessment of antiangiogenic treatment for wet age-related macular degeneration. Optom. Vis. Sci. 88:1255–1261. http://dx.doi.org/10.1097/OPX.0b013e3182282f13.

Baseler, H.A., Gouws, A., Haak, K.V., Racey, C., Crossland, M.D., Tufail, A., Rubin, G.S., Cornelissen, F.W., Morland, A.B., 2011b. Large-scale remapping of visual cortex is absent in adult humans with macular degeneration. Nat. Neurosci. 14:649–655. http://dx.doi.org/10.1038/nn.2793.

Bittner, A.K., Ibrahim, M.A., Haythornthwaite, J.A., Diener-West, M., Dagnelie, G., 2011. Vision test variability in retinitis pigmentosa and psychosocial factors. Optom. Vis. Sci. 88:1496–1506. http://dx.doi.org/10.1097/OPX.0b013e3182348d0b.

Bogorodzki, P., Piątkowska-Janko, E., Szaflik, J., Szaflik, J.P., Gacek, M., Grieb, P., 2014. Mapping cortical thickness of the patients with unilateral end-stage open angle glaucoma on planar cerebral cortex maps. PLoS One 9, e93682. doi:10.1371/journal.pone.0093682

Boldt, R., Seppä, M., Malinen, S., Tikka, P., Hari, R., Carlson, S., 2014. Spatial variability of functional brain networks in early-blind and sighted subjects. NeuroImage 95: 208–216. http://dx.doi.org/10.1016/j.neuroimage.2014.03.058.

Botelho, E.P., Ceriatte, C., Soares, J.G.M., Gattass, R., Fiorani, M., 2014. Quantification of early stages of cortical reorganization of the topographic map of V1 following retinal lesions in monkeys. Cereb. Cortex 24:1–16. http://dx.doi.org/10.1093/cercor/bhs208.

Boucard, C.C., Hernowo, A.T., Maguire, R.P., Jansonius, N.M., Roerdink, J.B.T.M., Hooymans, J.M.M., Cornelissen, F.W., 2009. Changes in cortical grey matter density associated with long-standing retinal visual field defects. Brain 132:1898–1906. http://dx.doi.org/10.1093/brain/awp119.

Bressler, D.W., Silver, M.A., 2010. Spatial attention improves reliability of fMRI retinotopic mapping signals in occipital and parietal cortex. NeuroImage 53:526–533. http://dx.doi.org/10.1016/j.neuroimage.2010.06.063.

Büchel, C., Price, C., Frackowiak, R.S.J., Friston, K., 1998. Different activation patterns in the visual cortex of late and congenitally blind subjects. Brain 121:409–419. http://dx.doi.org/10.1093/brain/121.3.409.

Burge, W.K., Griffis, J.C., Nenert, R., Elkhetali, A., DeCarlo, D.K., ver Hoef, L.W., Ross, L.A., Visscher, K.M., 2016. Cortical thickness in human V1 associated with central vision loss. Sci. Rep. 6:23268. http://dx.doi.org/10.1038/srep23268.

Burnat, K., 2015. Are visual peripheries forever young? Hindawi Publ. Corp.:1–13 http://dx.doi.org/10.1155/2015/307929.

Butz, M., van Ooyen, A., 2013. A simple rule for dendritic spine and axonal bouton formation can account for cortical reorganization after focal retinal lesions. PLoS Comput. Biol. 9:e1003259. http://dx.doi.org/10.1371/journal.pcbi.1003259.
Chen, W.W., Wang, N., Cai, S., Fang, Z., Yu, M., Wu, Q., Tang, L., Guo, B., Feng, Y., Jonas, J.B., Chen, X., Liu, X., Gong, Q., 2013. Structural brain abnormalities in patients with primary open-angle glaucoma: a study with 3 T MR imaging. Invest. Ophthalmol. Vis. Sci. 54:545–554. http://dx.doi.org/10.1167/iovs.12-9893.
Cheung, S.-H., Legge, G.E., 2005. Functional and cortical adaptations to central vision loss. Vis. Neurosci. 22:187–201. http://dx.doi.org/10.1017/S0952523805222071.
Cnaan, A., Laird, N.M., Slasor, P., 1997. Using the general linear mixed model to analyse unbalanced repeated measures and longitudinal data. Stat.Med. 16:2349–2380. http://dx.doi.org/10.1002/(SICI)1097-0258(19971030)16:20<2349::AID-SIM667>3.0.CO;2-E [pii].
Crossland, M.D., Morland, A.B., Feely, M.P., von dem Hagen, E., Rubin, G.S., 2008. The effect of age and fixation instability on retinotopic mapping of primary visual cortex. Invest. Ophthalmol. Vis. Sci. 49:3734–3739. http://dx.doi.org/10.1167/iovs.07-1621.
Cunningham, S.I., Shi, Y., Weiland, J.D., Falabella, P., Koo, C.O.D., Zacks, D.N., Tjan, B.S., 2015. Feasibility of structural and functional MRI acquisition with unpowered implants in argus II retinal prosthesis patients : a case study. Transl. Vis. Sci. Technol. 4:1–13. http://dx.doi.org/10.1167/tvst.4.6.6.
Dai, H., Morelli, J.N., Ai, F., Yin, D., Hu, C., Xu, D., Li, Y., 2012. Resting-state functional MRI: functional connectivity analysis of the visual cortex in primary open-angle glaucoma patients. Hum. Brain Mapp. 34:2455–2463. http://dx.doi.org/10.1002/hbm.22079.
d'Almeida, O.C., Mateus, C., Reis, A., Grazina, M.M., Castelo-Branco, M., 2013. Long term cortical plasticity in visual retinotopic areas in humans with silent retinal ganglion cell loss. NeuroImage 81:222–230. http://dx.doi.org/10.1016/j.neuroimage.2013.05.032.
Darian-Smith, C., Gilbert, C.D., 1995. Topographic reorganization in the striate cortex of the adult cat and monkey is cortically mediated. J. Neurosci. 15, 1631–1647.
D'Esposito, M., Deouell, L., Gazzaley, A., 2003. Alterations in the BOLD fMRI signal with ageing and disease: a challenge for neuroimaging. Nat. Rev. Neurosci. 4:1–11. http://dx.doi.org/10.1038/nrnXXX.
Dietrich, S., Hertrich, I., Ackermann, H., 2013. Ultra-fast speech comprehension in blind subjects engages primary visual cortex, fusiform gyrus, and pulvinar – a functional magnetic resonance imaging (fMRI) study. BMC Neurosci. 14:74. http://dx.doi.org/10.1186/1471-2202-14-74.
Dilks, D.D., Baker, C.I., Peli, E., Kanwisher, N., 2009. Reorganization of visual processing in macular degeneration is not specific to the "preferred retinal locus". J. Neurosci. 29:2768–2773. http://dx.doi.org/10.1523/JNEUROSCI.5258-08.2009.
Dilks, D.D., Julian, J.B., Peli, E., Kanwisher, N., 2014. Reorganization of visual processing in age-related macular degeneration depends on foveal loss. Optom. Vis. Sci. 91:e199–e206. http://dx.doi.org/10.1097/OPX.0000000000000325.
Duncan, R.O., Boynton, G.M., 2003. Cortical magnification within human primary visual cortex correlates with acuity thresholds. Neuron 38:659–671. http://dx.doi.org/10.1016/S0896-6273(03)00265-4.
Duncan, R.O., Sample, P.A., Weinreb, R.N., Bowd, C., Zangwill, L.M., 2007a. Retinotopic organization of primary visual cortex in glaucoma: comparing fMRI measurements of cortical function with visual field loss. Prog. Retin. Eye Res. 26:38–56. http://dx.doi.org/10.1016/j.preteyeres.2006.10.001.
Duncan, R.O., Sample, P.A., Weinreb, R.N., Bowd, C., Zangwill, L.M., 2007b. Retinotopic organization of primary visual cortex in glaucoma: a method for comparing cortical function with damage to the optic disk. Invest. Ophthalmol. Vis. Sci. 48:733–744. http://dx.doi.org/10.1167/iovs.06–0773.
Engel, S.A., Morland, A.B., Haak, K.V., 2015. Plasticity, and its limits, in adult human primary visual cortex. Multisens. Res. 28:297–307. http://dx.doi.org/10.1163/22134808-00002496.
Engelhorn, T., Michelson, G., Waerntges, S., Struffert, T., Haider, S., Doerfler, A., 2011. Diffusion tensor imaging detects rarefaction of optic radiation in glaucoma patients. Acad. Radiol. 18:764–769. http://dx.doi.org/10.1016/j.acra.2011.01.014.
Engin, K.N., Yemişci, B., Bayramoğlu, S.T., Güner, N.T., Özyurt, O., Karahan, E., Öztürk, C., Çağatay, P., 2014. Structural and functional evaluation of glaucomatous neurodegeneration from eye to visual cortex using 1.5 T MR imaging: a pilot study. J. Clin. Exp. Ophthalmol. 5:1–8. http://dx.doi.org/10.4172/2155-9570.1000341.
Erika, K.S., Guilherme, W., Christiane, K., Christa, N., Anja, I., Kober, S.E., Wood, G., Kampl, C., Neuper, C., Ischebeck, A., 2014. Electrophysiological correlates of mental navigation in blind and sighted people. Behav. Brain Res. 273:1–10. http://dx.doi.org/10.1016/j.bbr.2014.07.022.
Espinosa, J.S., Stryker, M.P., 2012. Development and plasticity of the primary visual cortex. Neuron 75:230–249. http://dx.doi.org/10.1016/j.neuron.2012.06.009.
Giannikopoulos, D.V., Eysel, U.T., 2006. Dynamics and specificity of cortical map reorganization after retinal lesions. Proc. Natl. Acad. Sci. U. S. A. 103:10805–10810. http://dx.doi.org/10.1073/pnas.0604539103.
Gilbert, C.D., Li, W., 2012. Adult visual cortical plasticity. Neuron 75:250–264. http://dx.doi.org/10.1016/j.neuron.2012.06.030.
Goesaert, E., Van Baelen, M., Spileers, W., Wagemans, J., Op de Beeck, H.P., 2014. Visual space and object space in the cerebral cortex of retinal disease patients. PLoS One 9:e88248. http://dx.doi.org/10.1371/journal.pone.0088248.
Gupta, N., Ang, L.-C., Noël de Tilly, L., Bidaisee, L., Yücel, Y.H., 2006. Human glaucoma and neural degeneration in intracranial optic nerve, lateral geniculate nucleus, and visual cortex. Br. J. Ophthalmol. 90:674–678. http://dx.doi.org/10.1136/bjo.2005.086769.
Gupta, N., Greenberg, G., de Tilly, L.N., Gray, B., Polemidiotis, M., Yücel, Y.H., 2009. Atrophy of the lateral geniculate nucleus in human glaucoma detected by magnetic resonance imaging. Br. J. Ophthalmol. 93:56–60. http://dx.doi.org/10.1136/bjo.2008.138172.
Haak, K.V., Cornelissen, F.W., Morland, A.B., 2012. Population receptive field dynamics in human visual cortex. PLoS One 7:e37686. http://dx.doi.org/10.1371/journal.pone.0037686.
Hamel, C., 2006. Retinitis pigmentosa. Orphanet J. Rare Dis. 1:40. http://dx.doi.org/10.1186/1750-1172-1-40.
Hartong, D.T., Berson, E.L., Dryja, T.P., 2006. Retinitis pigmentosa. Lancet 368:1795–1809. http://dx.doi.org/10.1016/S0140-6736(06)69740-7.
Hernowo, A.T., Prins, D., Baseler, H.A., Plank, T., Gouws, A.D., Hooymans, J.M.M., Morland, A.B., Greenlee, M.W., Cornelissen, F.W., 2014. Morphometric analyses of the visual pathways in macular degeneration. Cortex 56:99–110. http://dx.doi.org/10.1016/j.cortex.2013.01.003.
Holladay, J.T., 1997. Proper method for calculating average visual acuity. J. Refract. Surg.
Jacobson, S.G., Roman, A.J., Aleman, T.S., Sumaroka, A., Herrera, W., Windsor, E.A.M., Atkinson, L.A., Schwartz, S.B., Steinberg, J.D., Cideciyan, A.V., 2010. Normal central retinal function and structure preserved in retinitis pigmentosa. Invest. Ophthalmol. Vis. Sci. 51:1079–1085. http://dx.doi.org/10.1167/iovs.09-4372.
Jiang, J., Zhu, W., Shi, F., Liu, Y., Li, J., Qin, W., Li, K., Yu, C., Jiang, T., 2009. Thick visual cortex in the early blind. J. Neurosci. 29:2205–2211. http://dx.doi.org/10.1523/JNEUROSCI.5451-08.2009.
Kitajima, M., Korogi, Y., Hirai, T., Hamatake, S., Ikushima, I., Sugahara, T., Shigematsu, Y., Takahashi, M., Mukuno, K., 1997. MR changes in the calcarine area resulting from retinal degeneration. AJNR Am. J. Neuroradiol. 18:1291–1295. http://dx.doi.org/10.1097/00041327-199906000-00010.
Kitsos, G., Zikou, A.K., Bagli, E., Kosta, P., Argyropoulou, M.I., 2009. Conventional MRI and magnetisation transfer imaging of the brain and optic pathway in primary open-angle glaucoma. Br. J. Radiol. 82:896–900. http://dx.doi.org/10.1259/bjr/55866125.
Klein, A., Tourville, J., 2012. 101 labeled brain images and a consistent human cortical labeling protocol. Front. Neurosci. 6:1–12. http://dx.doi.org/10.3389/fnins.2012.00171.
Lee, V.K., Nau, A.C., Laymon, C., Chan, K.C., Rosario, B.L., Fisher, C., 2014. Successful tactile based visual sensory substitution use functions independently of visual pathway integrity. Front. Hum. Neurosci. 8:291. http://dx.doi.org/10.3389/fnhum.2014.00291.
Lemos, J., Pereira, D., Castelo-Branco, M., 2016. Visual cortex plasticity following peripheral damage to the visual system: fMRI evidence. Curr. Neurol. Neurosci. Rep. 16:89. http://dx.doi.org/10.1007/s11910-016-0691-0.
Lešťák, J., Tintěra, J., 2011. Changes in the visual cortex in patients with high-tension glaucoma. J. Clin. Exp. Ophthalmol. 1:8–11. http://dx.doi.org/10.4172/2155-9570.S4-002.
Lešťák, J., Tintěra, J., Karel, I., Svatá, Z., Rozsíval, P., 2013. Functional magnetic resonance imaging in patients with the wet form of age-related macular degeneration. Neuro-Ophthalmology 37:192–197. http://dx.doi.org/10.3109/01658107.2013.819581.
Lewald, J., Getzmann, S., 2013. Ventral and dorsal visual pathways support auditory motion processing in the blind: evidence from electrical neuroimaging. Eur. J. Neurosci. 38:3201–3209. http://dx.doi.org/10.1111/ejn.12306.
Liu, T., Cheung, S.-H., Schuchard, R.A., Glielmi, C.B., Hu, X., He, S., Legge, G.E., 2010. Incomplete cortical reorganization in macular degeneration. Invest. Ophthalmol. Vis. Sci. 51:6826–6834. http://dx.doi.org/10.1167/iovs.09-4926.
Marik, S.A., Yamahachi, H., Meyer zum Alten Borgloh, S., Gilbert, C.D., 2014. Large-scale axonal reorganization of inhibitory neurons following retinal lesions. J. Neurosci. 34:1625–1632. http://dx.doi.org/10.1523/JNEUROSCI.4345-13.2014.
Martins Rosa, A., Silva, M.F., Ferreira, S., Murta, J., Castelo-Branco, M., 2013. Plasticity in the human visual cortex: an ophthalmology-based perspective. Biomed. Res. Int.:568354 http://dx.doi.org/10.1155/2013/568354.
Masuda, Y., Dumoulin, S.O., Nakadomari, S., Wandell, B.A., 2008. V1 projection zone signals in human macular degeneration depend on task, not stimulus. Cereb. Cortex 18:2483–2493. http://dx.doi.org/10.1093/cercor/bhm256.
Masuda, Y., Horiguchi, H., Dumoulin, S.O., Furuta, A., Miyauchi, S., Nakadomari, S., Wandell, B.A., 2010. Task-dependent V1 responses in human retinitis pigmentosa. Invest. Ophthalmol. Vis. Sci. 51:5356–5364. http://dx.doi.org/10.1167/iovs.09-4775.
Merabet, L.B., Pascual-Leone, A., 2010. Neural reorganization following sensory loss: the opportunity of change. Nat. Rev. Neurosci. 11:44–52. http://dx.doi.org/10.1038/nrn2758.
Musarella, M.A., Macdonald, I.M., 2011. Current concepts in the treatment of retinitis pigmentosa. J. Ophthalmol.:753547 http://dx.doi.org/10.1155/2011/753547.
Noppeney, U., Friston, K.J., Ashburner, J., Frackowiak, R., Price, C.J., 2005. Early visual deprivation induces structural plasticity in gray and white matter. Curr. Biol. 15:R488–R490. http://dx.doi.org/10.1016/j.cub.2005.06.053.
Oishi, A., Otani, A., Sasahara, M., Kurimoto, M., Nakamura, H., Kojima, H., Yoshimura, N., 2009. Retinal nerve fiber layer thickness in patients with retinitis pigmentosa. Eye (Lond) 23:561–566. http://dx.doi.org/10.1038/eye.2008.63.
Oishi, A., Ogino, K., Nakagawa, S., Makiyama, Y., Kurimoto, M., Otani, A., Yoshimura, N., 2013. Longitudinal analysis of the peripapillary retinal nerve fiber layer thinning in patients with retinitis pigmentosa. Eye (Lond) 27:597–604. http://dx.doi.org/10.1038/eye.2013.34.
Olivo, G., Melillo, P., Cocozza, S., D'Alterio, F.M., Prinster, A., Testa, F., Brunetti, A., Simonelli, F., Quarantelli, M., 2015. Cerebral involvement in stargardt's disease: a VBM and TBSS study. Investig. Ophthalmol. Vis. Sci. 56:7388–7397. http://dx.doi.org/10.1167/iovs.15-16899.
Pan, W.-J., Wu, G., Li, C.-X., Lin, F., Sun, J., Lei, H., 2007. Progressive atrophy in the optic pathway and visual cortex of early blind Chinese adults: a voxel-based morphometry magnetic resonance imaging study. NeuroImage 37:212–220. http://dx.doi.org/10.1016/j.neuroimage.2007.05.014.
Park, H.-J., Lee, J.D., Kim, E.Y., Park, B., Oh, M.-K., Lee, S., Kim, J.-J., 2009. Morphological alterations in the congenital blind based on the analysis of cortical thickness and surface area. NeuroImage 47:98–106. http://dx.doi.org/10.1016/j.neuroimage.2009.03.076.

Pascual-Leone, A., Amedi, A., Fregni, F., Merabet, L.B., 2005. The plastic human brain cortex. Annu. Rev. Neurosci. 28:377–401. http://dx.doi.org/10.1146/annurev.neuro.27.070203.144216.

Plank, T., Frolo, J., Brandl-Rühle, S., Renner, A.B., Hufendiek, K., Helbig, H., Greenlee, M.W., 2011. Gray matter alterations in visual cortex of patients with loss of central vision due to hereditary retinal dystrophies. NeuroImage 56:1556–1565. http://dx.doi.org/10.1016/j.neuroimage.2011.02.055.

Poggel, D.A., Toth, L.J., Kim, D.S., Rizzo III, J.F., 2007. Brain activation maps in patients with retinal degeneration (abstract). Invest. Ophthalmol. Vis. Sci. 48, 935.

Poggel, D.A., Toth, L.J., Kim, D., Rizzo, J.F., n.d. Brain activation patterns indicate different forms of visual cortex plasticity in response to central and peripheral blindness. Unpubl. Work.

Prins, D., Hanekamp, S., Cornelissen, F.W., 2016a. Structural brain MRI studies in eye diseases: are they clinically relevant? A review of current findings. Acta Ophthalmol. 94:113–121. http://dx.doi.org/10.1111/aos.12825.

Prins, D., Plank, T., Baseler, H.A., Gouws, A.D., Beer, A., Morland, A.B., Greenlee, M.W., Cornelissen, F.W., 2016b. Surface-based analyses of anatomical properties of the visual cortex in macular degeneration. PLoS One 11:e0146684. http://dx.doi.org/10.1371/journal.pone.0146684.

Ptito, M., Schneider, F.C.G., Paulson, O.B., Kupers, R., 2008. Alterations of the visual pathways in congenital blindness. Exp. Brain Res. 187:41–49. http://dx.doi.org/10.1007/s00221-008-1273-4.

Qing, G., Zhang, S., Wang, B., Wang, N., 2010. Functional MRI signal changes in primary visual cortex corresponding to the central normal visual field of patients with primary open-angle glaucoma. Invest. Ophthalmol. Vis. Sci. 51:4627–4634. http://dx.doi.org/10.1167/iovs.09-4834.

Rangaswamy, N.V., Patel, H.M., Locke, K.G., Hood, D.C., Birch, D.G., 2010. A comparison of visual field sensitivity to photoreceptor thickness in retinitis pigmentosa. Invest. Ophthalmol. Vis. Sci. 51:4213–4219. http://dx.doi.org/10.1167/iovs.09-4945.

Ruff, C.C., Bestmann, S., Blankenburg, F., Bjoertomt, O., Josephs, O., Weiskopf, N., Deichmann, R., Driver, J., 2008. Distinct causal influences of parietal versus frontal areas on human visual cortex: evidence from concurrent TMS-fMRI. Cereb. Cortex 18:817–827. http://dx.doi.org/10.1093/cercor/bhm128.

Sammons, R.P., Keck, T., 2015. Adult plasticity and cortical reorganization after peripheral lesions. Curr. Opin. Neurobiol. 35:136–141. http://dx.doi.org/10.1016/j.conb.2015.08.004.

Schoth, F., Burgel, U., Dorsch, R., Reinges, M.H.T., Krings, T., 2006. Diffusion tensor imaging in acquired blind humans. Neurosci. Lett. 398:178–182. http://dx.doi.org/10.1016/j.neulet.2005.12.088.

Schumacher, E.H., Jacko, J.A., Primo, S.A., Main, K.L., Moloney, K.P., Kinzel, E.N., Ginn, J., 2008. Reorganization of visual processing is related to eccentric viewing in patients with macular degeneration. Restor. Neurol. Neurosci. 26, 391–402.

Shao, Y., Keliris, G.A., Papanikolaou, A., Fischer, M.D., Zobor, D., Jägle, H., Logothetis, N.K., Smirnakis, S.M., 2013. Visual cortex organisation in a macaque monkey with macular degeneration. Eur. J. Neurosci. 38:3456–3464. http://dx.doi.org/10.1111/ejn.12349.

Shintani, K., Shechtman, D.L., Gurwood, A.S., 2009. Review and update: current treatment trends for patients with retinitis pigmentosa. Optometry 80:384–401. http://dx.doi.org/10.1016/j.optm.2008.01.026.

Smirnakis, S.M., Brewer, A.A., Schmid, M.C., Tolias, A.S., Schüz, A., Augath, M., Inhoffen, W., Wandell, B.A., Logothetis, N.K., 2005. Lack of long-term cortical reorganization after macaque retinal lesions. Nature 435:300–307. http://dx.doi.org/10.1038/nature03495.

Strasburger, H., Rentschler, I., Jüttner, M., 2011. Peripheral vision and pattern recognition: a review. J. Vis. 11:13. http://dx.doi.org/10.1167/11.5.13.

Sunness, J.S., Liu, T., Yantis, S., 2004. Retinotopic mapping of the visual cortex using functional magnetic resonance imaging in a patient with central scotomas from atrophic macular degeneration. Ophthalmology 111:1595–1598. http://dx.doi.org/10.1016/j.ophtha.2003.12.050.

Thibaut, M., Tran, T.H.C., Szaffarczyk, S., Boucart, M., 2014. The contribution of central and peripheral vision in scene categorization: a study on people with central vision loss. Vis. Res. 98:46–53. http://dx.doi.org/10.1016/j.visres.2014.03.004.

Thomas, C., Baker, C.I., 2013. Teaching an adult brain new tricks: a critical review of evidence for training-dependent structural plasticity in humans. NeuroImage 73:225–236. http://dx.doi.org/10.1016/j.neuroimage.2012.03.069.

Van der Stigchel, S., Bethlehem, R.A.I., Klein, B.P., Berendschot, T.T.J.M., Nijboer, T.C.W., Dumoulin, S.O., 2013. Macular degeneration affects eye movement behavior during visual search. Front. Psychol. 4:579. http://dx.doi.org/10.3389/fpsyg.2013.00579.

Van Soest, S., Westerveld, A., De Jong, P.T.V.M., Bleeker-Wagemakers, E.M., Bergen, A.A.B., 1999. Retinitis pigmentosa: defined from a molecular point of view. Surv. Ophthalmol. 43:321–334. http://dx.doi.org/10.1016/S0039-6257(98)00046-0.

Visscher, K., Nenert, R., DeCarlo, D., Chen, R., Ross, L., 2014. Macular degeneration affects functional connectivity of primary visual cortex. J. Vis. 14:956. http://dx.doi.org/10.1167/14.10.956.

Vossel, S., Geng, J.J., Fink, G.R., 2014. Dorsal and ventral attention systems: distinct neural circuits but collaborative roles. Neuroscientist 20:150–159. http://dx.doi.org/10.1177/1073858413494269.

Walia, S., Fishman, G.A., 2008. Retinal nerve fiber layer analysis in RP patients using Fourier-domain OCT. Invest. Ophthalmol. Vis. Sci. 49:3525–3528. http://dx.doi.org/10.1167/iovs.08-1842.

Walia, S., Fishman, G.A., Edward, D.P., Lindeman, M., 2007. Retinal nerve fiber layer defects in RP patients. Invest. Ophthalmol. Vis. Sci. 48:4748–4752. http://dx.doi.org/10.1167/iovs.07-0404.

Wandell, B.A., Smirnakis, S.M., 2009. Plasticity and stability of visual field maps in adult primary visual cortex. Nat. Rev. Neurosci. 10:873–884. http://dx.doi.org/10.1038/nrn2741.

Wandell, B.A., Dumoulin, S.O., Brewer, A.A., 2007. Visual field maps in human cortex. Neuron 56:366–383. http://dx.doi.org/10.1016/j.neuron.2007.10.012.

Wang, B., Yamamoto, H., 2013. Visual field maps of the human visual cortex for central and peripheral vision. Neurosci. Biomed. Eng. 1:102–110. http://dx.doi.org/10.2174/2213385202666140207002441.

Wang, D., Qin, W., Liu, Y., Zhang, Y., Jiang, T., Yu, C., 2014. Altered resting-state network connectivity in congenital blind. Hum. Brain Mapp. 35:2573–2581. http://dx.doi.org/10.1002/hbm.22350.

Weaver, K.E., Richards, T.L., Saenz, M., Petropoulos, H., Fine, I., 2013. Neurochemical changes within human early blind occipital cortex. Neuroscience 252:222–233. http://dx.doi.org/10.1016/j.neuroscience.2013.08.004.

Xie, J., Wang, G.J., Yow, L., Humayun, M.S., Weiland, J.D., Cela, C.J., Jadvar, H., Lazzi, G., Dhrami-Gavazi, E., Tsang, S.H., 2012. Preservation of retinotopic map in retinal degeneration. Exp. Eye Res. 98:88–96. http://dx.doi.org/10.1016/j.exer.2012.03.017.

Yamahachi, H., Marik, S.A., McManus, J.N.J., Denk, W., Gilbert, C.D., 2009. Rapid axonal sprouting and pruning accompany functional reorganization in primary visual cortex. Neuron 64:719–729. http://dx.doi.org/10.1016/j.neuron.2009.11.026.

Yu, L., Xie, B., Yin, X., Liang, M., Evans, A.C., Wang, J., Dai, C., 2013. Reduced cortical thickness in primary open-angle glaucoma and its relationship to the retinal nerve fiber layer thickness. PLoS One 8, e73208. doi:10.1371/journal.pone.0073208

Yu, L., Yin, X., Dai, C., Liang, M., Wei, L., Li, C., Zhang, J., Xie, B., Wang, J., 2014. Morphologic changes in the anterior and posterior subregions of V1 and V2 and the V5/MT+ in patients with primary open-angle glaucoma. Brain Res. 1588:135–143. http://dx.doi.org/10.1016/j.brainres.2014.09.005.

Zikou, A.K., Kitsos, G., Tzarouchi, L.C., Astrakas, L., Alexiou, G.A., Argyropoulou, M.I., 2012. Voxel-based morphometry and diffusion tensor imaging of the optic pathway in primary open-angle glaucoma: a preliminary study. Am. J. Neuroradiol. 33:128–134. http://dx.doi.org/10.3174/ajnr.A2714.

Renier, L., Cuevas, I., Grandin, C.B., Dricot, L., Plaza, P., Lerens, E., Rombaux, P., De Volder, A.G., 2013. Right occipital cortex activation correlates with superior odor processing performance in the early blind. PLoS One 8, e71907. http://dx.doi.org/10.1371/journal.pone.0071907.